Journal of the Korean Astronomical Society
55: 139 ∼ 148, 2022 October
https://doi.org/10.5303/JKAS.2022.55.5.139
pISSN: 1225-4614 · eISSN: 2288-890X
http://jkas.kas.org

Solar Activity and Latitudinal Distribution of Sunspots

Heon-Young Chang
Department of Astronomy and Atmospheric Sciences, Kyungpook National University, Daegu 41566, Republic of Korea; hyc@knu.ac.kr

Received May 12, 2022; accepted August 17, 2022

Abstract: We explore the latitudinal distribution of sunspots and pursue to establish a correlation between the statistical parameters of the latitudinal distribution of sunspots and characteristics of solar activity. For this purpose, we have statistically analyzed the daily sunspot areas and latitudes observed from May in 1874 to September in 2016. As results, we confirm that the maximum of the monthly averaged International Sunspot Number (ISN) strongly correlates with the mean number of sunspots per day, while the maximum ISN strongly anti-correlates with the number of spotless days. We find that both the maximum ISN and the mean number of sunspots per day strongly correlate with the the average latitude, the standard deviation, the skewness of the the latitudinal distribution of sunspots, while they appears to marginally correlate with the kurtosis. It is also found that the northern and southern hemispheres seem to show a correlated behavior in a different way when sunspots appearing in the northern and southern hemispheres are examined separately.

Key words: sunspots — Sun: activity — methods: data analysis

1. Introduction

Solar activity triggers changes in the Earth's system, which may threaten the human population in the world. The temporal variability of the solar magnetic field strength modulates the interplanetary space, in turn the terrestrial electromagnetical environment manifested in the disturbance storm time index, the Auroral Electrojet index, influx of energetic particles into the atmosphere (Garcia et al. 1984; Kane 2005; de Artigas et al. 2006; Prestes et al. 2006). Together with galactic cosmic ray penetrating into the troposphere, solar irradiance variability, such as, the total solar irradiance and extreme ultraviolet irradiance, links the solar magnetic activity to various climatic anomalies or some of extreme weather events (Tinsley 2000; Puovkin et al. 1997; Svensmark & Friis-Christensen 1997; Hathaway & Wilson 2004; Haigh 2007; Meehl et al. 2009; Roy & Haigh 2010; Cho et al. 2012; Mironova & Usoskin 2013; Gray et al. 2017; Kim & Chang 2019).

The solar magnetic variability is crucial in the field of theoretical solar research as well as practical applications. Suggested models of magnetic field generation should be constrained by the observed conditions. As sunspots form as soon as the magnetic tube emerges from the subsurface layer of the Sun, they can be considered as tracers of freshly emerged magnetic flux tubes (Pulkkinen et al. 1999). Given that sunspot observations provide the longest running direct records of solar activity, a temporal distribution of the observed sunspots as a proxy of solar activity has been carefully examined to establish empirical relations.

For example, solar activity with an ∼11 year periodicity is most well known, though every cycle is different from each other with its own amplitude, length and shape. Besides, there are also prolonged intervals of very low or high activity, which are referred to as grand minima and maxima (e.g., Usoskin 2017). Moreover, the solar maximum amplitude appears to anti-correlate with the duration of ascending phases of a solar cycle, known as the Waldmeier effect (Waldmeier 1935). The solar maximum amplitude for an odd cycle appears to correlate with the solar maximum amplitude of the preceding even cycle, known as the Gnevyshev-Ohl rule (Gnevyshev & Ohl 1948). However, we note that there are some exceptions to the Gnevyshev-Ohl rule for the pairs of cycle 4/5, 8/9 and 22/23 (e.g., Joshi et al. 2006).

Another example of notable features in solar activity is the solar North-South asymmetry. The asymmetry between the northern and southern hemispheres has been found in various indices of solar activity, such as, sunspot number, sunspot area, flare index (Waldmeier 1971; Roy 1977; White & Trotter 1977; Verma 1988, 1993; Javaraiah 2007; Li et al. 2002; Krivova & Solanki 2002; Zaatri et al. 2006; Joshi et al. 2015; Zharkova & Shepherd 2022). The solar North-South asymmetry appears periodic and to be related with the level of the activity (Chang 2018). Thus, the solar North-South asymmetry should be reproduced by details of the solar dynamo model in that such a spatial distribution of sunspots also provides invaluable information on the physical processes that induce its structure and evolution.

The latitude of the sunspot generating zone is also significant characteristic of the spatial distribution of emerged magnetic flux tubes. Sunspots of a new solar cycle begin to appear at latitudes of $\sim\pm40°$. As the solar cycle proceeds, the region of sunspot formation moves to the equator and the drift rate of the zone of spotting decreases (Carrington 1860). This behavior results in the butterfly diagram (Maunder 1904). A

systematic pattern in the orientation of sunspot groups was also noted by Hale et al. (1919). According to their findings, the leading sunspot in both hemispheres which have the opposite polarity tends to locate closer to the equator as compared with the following sunspot of the same group. The tilt angle, which is the angle between the spotting latitude and the line connecting the leading to following sunspots in a sunspot group, increases with latitude, referred to as Joy's law (e.g., Wang & Sheeley 1989; Howard 1991; Pevtsov et al. 2014).

Indeed, the observed butterfly diagram has been compared with a theoretical dynamo-model by testing if forming region of sunspots is properly drifting equatorward from latitudes of $\sim\pm40^\circ$ as observed (e.g., Hathaway 2011), or by statistically exploring the latitudinal variation of the location of sunspots with time (Temmer et al. 2002, 2006; Zolotova & Ponyavin 2006, 2007; Ternullo 2007, 2010; Li et al. 2010). In statistical investigation of the latitudinal distribution of sunspots, it has been found that stronger cycles begin at relatively higher latitudes with a wider latitudinal dispersion (Li et al. 2002; Solanki et al. 2008; Chang 2012). Interestingly enough, reported correlations are different in two hemispheres. One critical point that must be kept in mind is that all sunspots are dealt equally in those kinds of statistical study regardless of their lifetime, or size. Having studied its latitudinal distribution with the area-weighted butterfly diagram, Chang (2011, 2012, 2015, 2018) found that the latitude distribution of sunspots appears to follow a bimodal distribution and confirmed that the level of solar activity correlates with the median latitude of the spotting zone.

In this paper, we investigate the distribution of the latitude of sunspots in terms of descriptive statistics. To begin with, we ignore their temporal and spatial dimension for the time being as in a conventional approach. We first compute the statistical parameters for a given solar cycle directly relating to the 0th to 4th moments of the latitudinal distribution of sunspots to consider a shape of the distribution of the latitude of sunspots belonging to different solar cycles. Then, we attempt to establish a correlation between the statistical parameters of the latitude distribution of sunspots and characteristics of solar activity. The executed analysis has been repeatedly carried out for the sunspots appearing either in the northern hemisphere or in the southern hemisphere only. Here, unlike previous studies, we particularly include attributes of solar activity which are not yet sufficiently considered, such as, sunspot number per day, the number of spotless days. We also attempt to answer to a question of how the conclusion depends on the size of sunspots, which is another merit of this study. As we know that the butterfly diagram is dominated by small sunspots, statistical properties of the latitudinal distribution of the observed sunspots may well be suspected to be determined by small and numerous sunspots, not by large and rare sunspots. In fact, the half of the total spotted area is covered by less than $\sim$10% of groups (the largest ones), on the other hand, the smallest 65% of the sunspots contribute only up to $\sim$10% of the total sunspot area (Ternullo 2007).

This paper is organized as follows. We begin with a description of the data analyzed in the present paper and methods to obtain the statistical parameters of the distribution of the latitude of sunspots in Section 2. We present the relation among the solar activity parameters describing a solar cycle in Section 3, and discuss how the statistical parameters of the latitudinal distribution of sunspots are associated with the solar activity parameters in Section 4. Finally, we summarize the results and briefly conclude in Section 5.

2. DATA AND STATISTICAL PARAMETERS

We have used for the present analysis the daily sunspot areas and latitudes obtained from the NASA website[1]. The analysed data set covers from May in 1874 to September in 2016, spanning from the solar cycles 11 to 24. The observed sunspot data from the incomplete cycles 11 and 24 are used to determine the boundaries of the solar cycles 12 and 23, respectively. One ought to use them since sunspots cannot be allocated simply into a solar cycle in terms of the date of the official minimum of the sunspot cycles. Indeed, such a naive criterion is hardly accepted in isolating sunspots for a given solar cycle in researches of similar purpose of this paper (e.g., Li et al. 2002; Solanki et al. 2008).

The following is how we define the boundary between consecutive solar cycles. In Figure 1, we show the butterfly diagram, in which it can be noticed that the sunspot cycles overlap each other. That is, the first sunspots of a new cycle appear at high latitudes, whereas the last sunspots of an old cycle still appear near the equator. Hence, sunspots at low latitudes in the ascending phase of a cycle should not be counted since they are to be identified as belongings to the previous solar cycle. Similarly, sunspots at high latitudes in the descending phase should not be counted since they are regarded as belongings to the following solar cycle. Thus, the provisional boundaries between cycles have been estimated by looking for the one year wide interval for which the number of sunspots is smallest at each latitude. Then, an inclined straight line starting at the point where the latitude-axis coordinate value is 0 and the time-coordinate value is the minimum times is fit separately for both hemispheres. As a result, this straight-line is adopted as the boundary between solar cycles. As an example, we show the boudaries between the solar cycles 23 and 24 for both hemispheres with the inclined dashed line in Figure 1. As seen in Figure 1, the position of boundaries obtained by such a manner is usually unambiguous.

Having assigned the boundary between consecutive solar cycles, we compute the latitudinal distribution of the observed sunspots for a specific solar cycle by summing the butterfly diagram at each latitude bin over each cycle. In Figure 2, we show the probability function of the latitudinal distribution of the observed sunspots normalized such that the total area of the

[1] http://solarscience.msfc.nasa.gov/greenwch.shtml

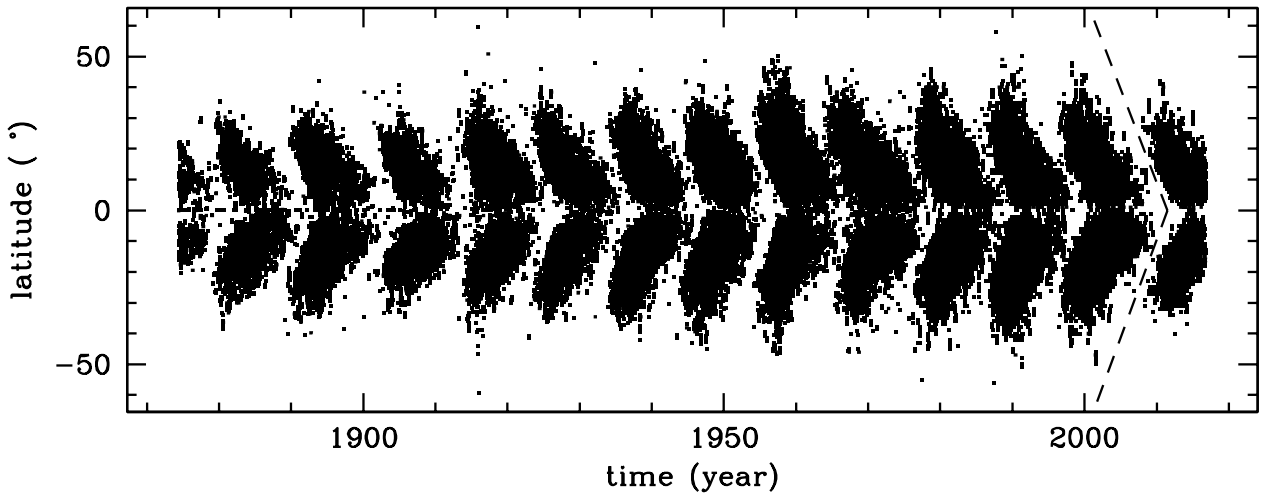

Figure 1. Butterfly diagram constructed with the observed sunspots from May in 1874 to September in 2016, spanning from the solar cycles 11 to 24. The latitude of the northern and southern hemispheres is denoted by '+' and '−' signs, respectively.

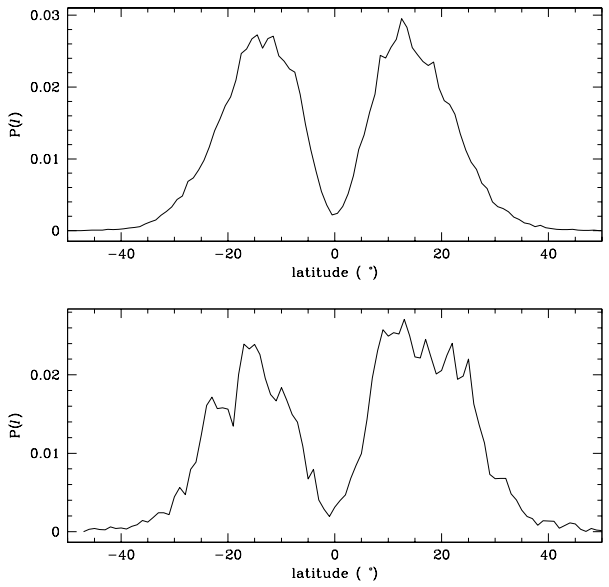

Figure 2. Latitudinal distribution of the observed sunspots. In the upper panel, the normalized latitudinal distribution of the sunspots observed from solar cycles 12 to 23, $P(l)$, is shown. In the lower panel, $P(l)$ of the solar cycle 19 is shown, as an example of the normalized latitudinal distribution resulting from a single solar cycle.

function is unity. In the upper panel, the normalized latitudinal distribution of the sunspots observed from solar cycles 12 to 23, $P(l)$, is presented. In the lower panel, as an example of the normalized latitudinal distribution resulting from the observed sunspots during a single solar cycle, $P(l)$ of the strongest solar cycle 19 is illustrated. The positive and negative latitudes stand for the northern and southern hemispheres, respectively.

With the latitudinal distribution of the observed sunspots for each of the solar cycles 12 to 23, we form the five lowest moments of the latitudinal distribution of sunspots, respectively. The five lowest moments are defined as

$$m_0 = \int_{0^\circ}^{90^\circ} P(l)\ dl, \tag{1}$$

$$m_1 = \frac{1}{m_0} \int_{0^\circ}^{90^\circ} P(l)\,|l|\ dl, \tag{2}$$

$$m_i = \frac{1}{m_0} \int_{0^\circ}^{90^\circ} P(l)\,|(l - m_1)|^i\ dl, \tag{3}$$

with $i = 2, 3, 4$, where $P(l)$ is the normalized latitudinal distribution of the observed sunspots and l is the latitude. Note that there are practically no sunspots above $\sim\pm60^\circ$. Now, the statistical parameters are related to the obtained moments as follows:

$$A = m_1, \tag{4}$$

$$\sigma = \sqrt{m_2}, \tag{5}$$

$$s = \frac{m_3}{\sigma^3}, \tag{6}$$

$$k = \frac{m_4}{\sigma^4} - 3. \tag{7}$$

Here, A and σ correspond to the average latitude at which sunspots are commonly located during a given cycle, and the standard deviation measuring a width of the latitudinal distribution of sunspots. Parameters s and k correspond to the skewness and the kurtosis, both of which describe the shape of the distribution. In other words, the skewness is zero when the profile is symmetric and positive if the profile is skewed more towards the equator. By definition, the kurtosis is zero for a Gaussian profile, positive for a more peaked profile and negative for a more box-like profile. Basically, we have done computations for the two hemispheres,

Table 1
Correlation coefficients of solar activity parameters

	r	r_s	τ
maximum ISN vs spots per day	0.97 (2.4×10^{-7})	0.97 (1.3×10^{-7})	0.91 (3.9×10^{-5})
maximum ISN vs time of rise	−0.49 (0.107)	−0.58 (0.047)	−0.38 (0.089)
maximum ISN vs duration	−0.45 (0.152)	−0.33 (0.295)	−0.18 (0.403)
maximum ISN vs spotless days	−0.75 (0.005)	−0.77 (0.003)	−0.64 (0.004)
spots per day vs time of rise	−0.55 (0.064)	−0.57 (0.052)	−0.38 (0.090)
spots per day vs duration	−0.47 (0.119)	−0.37 (0.243)	−0.22 (0.330)
spots per day vs spotless days	−0.85 (4.5×10^{-4})	−0.87 (2.6×10^{-4})	−0.73 (0.001)
time of rise vs duration	0.57 (0.052)	0.45 (0.141)	0.38 (0.085)
time of rise vs spotless days	0.49 (0.104)	0.56 (0.059)	0.41 (0.066)
duration vs spotless days	0.55 (0.064)	0.45 (0.143)	0.25 (0.265)

Linear correlation coefficient r, a Spearman rank-order correlation value r_s, and Kendall's τ, resulting from combinations of the maximum of the monthly averaged International Sunspot Number (maximum ISN), the duration defined by minimum-to-minimum (duration), the duration of ascending phase (time of rise), the mean number of sunspots per day (spots per day), the number of spotless days (spotless days). Rejection probabilities are included in parentheses.

separately. For results of the sunspots appearing in the two hemisphere, we use unsigned latitudes of the observed the sunspots appearing in both hemispheres. Note that in some previous reports studying moments of the distribution the total m_i is simply defined as an arithmetic average of moments resulting from two hemispheres: $m_i = (m_{i,N} + m_{i,S})/2$ (e.g., Solanki et al. 2008).

3. TEMPORAL DISTRIBUTION

Before investigating the statistical parameters of the latitudinal distribution of sunspots, we first examine the relationship among the solar activity parameters describing a solar cycle, such as, the maximum of the monthly averaged International Sunspot Number (ISN) available at SILSO[2], the total duration defined by minimum-to-minimum, the duration of ascending phase from the starting minimum to the maximum for a given solar cycle, the mean number of sunspots per day, the number of spotless days. We calculate Pearson's linear correlation coefficient r and the single-sided probability that $|r|$ has an equal or greater value than its observed in the null hypothesis, which are listed in Table 1.

We find that the maximum ISN highly correlates with the mean number of sunspots per day, while the maximum ISN highly anti-correlates with the number of spotless days. Not surprisingly, the mean number of sunspots per day highly anti-correlates with the number of spotless days. In the meantime, the maximum ISN marginally anti-correlates with the total durations and the duration of ascending phase, which is expected from the Waldmeier effect. In addition, the number of spotless days also marginally correlates with both the total durations and the duration of ascending phase. To perform supplementary statistical tests of data sets, we have carried out the Spearman rank-order correlation test, returning a correlation coefficient r_s and the single-sided chance probability $P(r_s, N)$ that N pairs of uncorrelated variables would yield a value of r_s equally or more discrepant than the one obtained from the data set. We have also calculated Kendall's τ and the chance probability P_τ whose meaning is similar to that of $P(r_s, N)$. While Pearson's correlation assumes linear relationships between variables, Spearman's correlation assesses monotonic relationships whether or not the variables are linear. Spearman's rank correlation basically gives the measure of monotonicity of the relation between variables. Furthermore, the Kendall rank correlation coefficient is a statistic used to measure the ordinal association between two measured quantities, which is the relationship between rankings of different ordinal variables. General trends of test results are similar to those of the Pearson's linear correlation test. The results of non-parametric hypothesis tests are also listed in Table 1.

[2] http://sidc.be/silso/datafiles

4. LATITUDINAL DISTRIBUTION

In Table 2, we list the correlation coefficients with the rejection probability resulting from combinations of the average latitude, the standard deviation, the skewness, and the kurtosis. All the statistical parameters are calculated with data sets of the sunspots appearing in both hemispheres. Based on linear correlation coefficients r summarized in Table 2, all the statistical parameters correlate remarkably with each other in general. It is found, in particular, that the average latitude highly correlate with both the standard deviation and the skewness, and that the skewness highly correlate with both the standard deviation and the kurtosis. While, the kurtosis marginally correlate with the average latitude and the standard deviation with somewhat high chance probabilities. It is interesting to note that correlations coefficients between the average latitude and the standard deviation are nearly 1 with 0 chance probability. That is, for a solar cycle with the center of wings of a higher (lower) latitude, its wing is naturally broad (narrow) and yet peaked (boxy) towards the lower latitude in the butterfly diagram. This

Table 2
Correlation coefficients of statistical parameters

	r	r_s	τ
$A_{\rm all}$ vs $\sigma_{\rm all}$	0.99 (4.5×10^{-10})	0.99 (4.1×10^{-9})	0.94 (2.1×10^{-5})
$A_{\rm all}$ vs $s_{\rm all}$	0.77 (0.003)	0.62 (0.031)	0.39 (0.070)
$A_{\rm all}$ vs $k_{\rm all}$	0.49 (0.104)	0.38 (0.217)	0.24 (0.272)
$\sigma_{\rm all}$ vs $s_{\rm all}$	0.83 (0.001)	0.64 (0.026)	0.45 (0.039)
$\sigma_{\rm all}$ vs $k_{\rm all}$	0.47 (0.119)	0.39 (0.199)	0.24 (0.272)
$s_{\rm all}$ vs $k_{\rm all}$	0.60 (0.037)	0.52 (0.080)	0.42 (0.055)

Linear correlation coefficient r, a Spearman rank-order correlation value r_s, and Kendall's τ, resulting from combinations of the average latitude (A), the standard deviation (σ), the skewness (s), and the kurtosis (k), all of which are calculated with data sets of the sunspots appearing in both hemispheres. Rejection probabilities are included in parentheses.

Table 3
Correlation coefficients of latitude distribution of sunspots and characteristics of solar activity

	r	r_s	τ
maximum ISN vs $A_{\rm all}$	0.89 (8.4×10^{-5})	0.90 (5.9×10^{-5})	0.75 (0.001)
maximum ISN vs $\sigma_{\rm all}$	0.88 (1.5×10^{-4})	0.90 (5.9×10^{-5})	0.76 (0.001)
maximum ISN vs $s_{\rm all}$	0.70 (0.011)	0.64 (0.026)	0.45 (0.039)
maximum ISN vs $k_{\rm all}$	0.59 (0.043)	0.58 (0.048)	0.42 (0.054)
spots per day vs $A_{\rm all}$	0.91 (4.2×10^{-5})	0.91 (4.1×10^{-5})	0.79 (0.001)
spots per day vs $\sigma_{\rm all}$	0.91 (3.7×10^{-5})	0.91 (4.2×10^{-5})	0.79 (0.001)
spots per day vs $s_{\rm all}$	0.79 (0.002)	0.69 (0.011)	0.54 (0.013)
spots per day vs $k_{\rm all}$	0.55 (0.065)	0.53 (0.075)	0.33 (0.131)
time of rise vs $A_{\rm all}$	−0.35 (0.263)	−0.45 (0.141)	−0.34 (0.119)
time of rise vs $\sigma_{\rm all}$	−0.32 (0.304)	−0.42 (0.174)	−0.28 (0.202)
time of rise vs $s_{\rm all}$	−0.28 (0.377)	−0.39 (0.199)	−0.28 (0.202)
time of rise vs $k_{\rm all}$	−0.11 (0.733)	−0.15 (0.645)	−0.09 (0.671)
duration vs $A_{\rm all}$	−0.33 (0.302)	−0.24 (0.455)	−0.15 (0.486)
duration vs $\sigma_{\rm all}$	−0.35 (0.266)	−0.29 (0.358)	−0.17 (0.256)
duration vs $s_{\rm all}$	−0.34 (0.295)	−0.18 (0.578)	−0.12 (0.577)
duration vs $k_{\rm all}$	−0.07 (0.824)	−0.09 (0.778)	−0.06 (0.782)
spotless days vs $A_{\rm all}$	−0.84 (0.001)	−0.84 (6.4×10^{-4})	−0.69 (0.001)
spotless days vs $\sigma_{\rm all}$	−0.88 (2.3×10^{-4})	−0.84 (0.001)	−0.69 (0.001)
spotless days vs $s_{\rm all}$	−0.89 (7.0×10^{-5})	−0.67 (0.017)	−0.52 (0.019)
spotless days vs $k_{\rm all}$	−0.47 (0.128)	−0.37 (0.236)	−0.24 (0.272)

Linear correlation coefficient r, a Spearman rank-order correlation value r_s, and Kendall's τ, calculated with the solar activity parameters and the statistical parameters of the latitudinal distribution of the observed sunspots. Note that the statistical parameters are calculated with data sets of the sunspots appearing in both hemispheres. Rejection probabilities are included in parentheses.

profile of the latitudinal distribution becomes possible when the first sunspots of a new cycle begin to emerge at much higher (relatively lower) latitudes and sunspots crowd the lower (almost uniformly) latitude region.

To investigate how the statistical parameters of the latitudinal distribution of sunspots are associated with the solar activity parameters, we calculate the correlation coefficients with the rejection probability between the solar activity parameters and the statistical parameters of the latitudinal distribution of the observed sunspots and summarize the results in Table 3. As shown in Table 3, both the maximum ISN and the mean number of sunspots per day highly correlate with the statistical parameters relating to the 1st to 3rd moments of the distribution function, even though they appears to marginally correlate with the kurtosis. What it implies is that when the solar cycle is strong the profiles are skewed such that the latitudinal distribution is peaked closer to the equator while sunspots are distributed in a long tail at higher latitudes. This finding is confirmed with the number of spotless days. The number of spotless days show similar behaviors, except that they are anti-correlated. As for the total duration and the duration of ascending phase, however, rejection probability is too high to draw any statistical conclusions.

As pointed out above, the northern and southern hemispheres behave rather differently due to the North-South asymmetry of solar activity. Consequently, our focus moves to test if statistical tendency is reproduced when the statistical parameters are calculated using the sunspots appearing in the northern and southern

Table 4
Correlation coefficients of statistical parameters from each hemisphere

	r	r_s	τ
A_N vs σ_N	0.95 (0.002)	0.94 (3.9×10^{-6})	0.82 (0.001)
A_N vs s_N	0.08 (0.804)	−0.23 (0.471)	−0.12 (0.583)
A_N vs k_N	−0.17 (0.601)	0.08 (0.795)	0.16 (0.492)
σ_N vs s_N	0.23 (0.466)	−0.02 (0.948)	0.01 (0.973)
σ_N vs k_N	−0.02 (0.942)	0.21 (0.512)	0.16 (0.493)
s_N vs k_N	0.71 (0.010)	0.72 (0.008)	0.61 (0.006)
A_S vs σ_S	0.88 (0.001)	0.91 (4.1×10^{-5})	0.75 (0.001)
A_S vs s_S	0.51 (0.091)	0.47 (0.124)	0.30 (0.170)
A_S vs k_S	0.45 (0.142)	0.44 (0.151)	0.30 (0.170)
σ_S vs s_S	0.77 (0.003)	0.67 (0.017)	0.48 (0.028)
σ_S vs k_S	0.41 (0.188)	0.37 (0.226)	0.24 (0.272)
s_S vs k_S	0.51 (0.092)	0.53 (0.075)	0.39 (0.074)

Similar to Table 2, linear correlation coefficient r, a Spearman rank-order correlation value r_s, and Kendall's τ, resulting from combinations of the average latitude (A), the standard deviation (σ), the skewness (s), and the kurtosis (k), except that these statistical parameters are due to the sunspots appearing only in one hemisphere.

Table 5
Correlation coefficients of solar activity parameters and statistical parameters from the northern hemisphere

	r	r_s	τ
maximum ISN vs A_N	0.82 (0.001)	0.82 (0.001)	0.67 (0.003)
maximum ISN vs σ_N	0.80 (0.002)	0.75 (0.005)	0.61 (0.006)
maximum ISN vs s_N	0.28 (0.375)	0.03 (0.914)	0.03 (0.891)
maximum ISN vs k_N	0.13 (0.688)	0.27 (0.391)	0.18 (0.410)
spots per day vs A_N	0.87 (0.001)	0.86 (0.001)	0.70 (0.002)
spots per day vs σ_N	0.82 (0.001)	0.80 (0.001)	0.64 (0.003)
spots per day vs s_N	0.28 (0.371)	0.03 (0.931)	0.01 (0.987)
spots per day vs k_N	0.02 (0.959)	0.23 (0.470)	0.15 (0.492)
time of rise vs A_N	−0.26 (0.411)	−0.35 (0.260)	−0.25 (0.258)
time of rise vs σ_N	−0.21 (0.515)	−0.19 (0.558)	−0.13 (0.571)
time of rise vs s_N	−0.08 (0.796)	0.13 (0.678)	0.09 (0.671)
time of rise vs k_N	0.17 (0.601)	−0.27 (0.393)	0.19 (0.396)
duration vs A_N	−0.24 (0.446)	−0.14 (0.671)	−0.06 (0.780)
duration vs σ_N	−0.39 (0.208)	−0.28 (0.388)	−0.18 (0.403)
duration vs s_N	−0.40 (0.203)	−0.21 (0.511)	−0.15 (0.486)
duration vs k_N	−0.11 (0.739)	0.09 (0.761)	0.13 (0.577)
spotless days vs A_N	−0.84 (0.001)	−0.86 (0.001)	−0.73 (0.001)
spotless days vs σ_N	−0.83 (0.001)	−0.85 (0.001)	−0.67 (0.002)
spotless days vs s_N	−0.29 (0.363)	0.09 (0.779)	0.09 (0.680)
spotless days vs k_N	0.02 (0.953)	−0.04 (0.879)	−0.06 (0.783)

Similar to Table 3, linear correlation coefficient r, a Spearman rank-order correlation value r_s, and Kendall's τ, calculated with the solar activity parameters and the statistical parameters of the latitudinal distribution of the observed sunspots only in the northern hemispheres.

hemispheres, respectively. In Table 4, similar to Table 2, we list the correlation coefficients with the rejection probability resulting from combinations of the average latitude, the standard deviation, the skewness, and the kurtosis due to the sunspots appearing only in one hemisphere. Significant correlations between the average latitude and the standard deviation, and between the skewness and the kurtosis are recovered in both hemispheres. On the other hand, the correlated behavior between the standard deviation and the skewness can be found from the sunspots appearing in the southern hemisphere, but not in the northern hemisphere. Accordingly, when the correlation coefficients between the solar activity parameters and the statistical parameters are calculated with the sunspots appearing in the northern and southern hemispheres separately, it is found that the correlated behavior between the skewness and the solar activity parameters becomes weaker. In particular, it is difficult to determine whether they are statistically correlated based on the sunspots in the

Table 6
Correlation coefficients of solar activity parameters and statistical parameters from the southern hemisphere

	r	r_s	τ
maximum ISN vs A_S	0.91 (4.1×10^{-5})	0.93 (1.1×10^{-5})	0.81 (0.001)
maximum ISN vs σ_S	0.86 (0.001)	0.89 (8.4×10^{-5})	0.75 (0.001)
maximum ISN vs s_S	0.51 (0.090)	0.57 (0.051)	0.36 (0.099)
maximum ISN vs k_S	0.54 (0.068)	0.54 (0.071)	0.36 (0.099)
spots per day vs A_S	0.87 (0.001)	0.86 (0.001)	0.72 (0.001)
spots per day vs σ_S	0.89 (0.001)	0.89 (0.001)	0.72 (0.001)
spots per day vs s_S	0.63 (0.030)	0.66 (0.018)	0.45 (0.039)
spots per day vs k_S	0.54 (0.072)	0.55 (0.062)	0.39 (0.074)
time of rise vs A_S	−0.43 (0.165)	−0.49 (0.105)	−0.37 (0.089)
time of rise vs σ_S	−0.39 (0.216)	−0.51 (0.089)	−0.41 (0.066)
time of rise vs s_S	−0.19 (0.549)	−0.38 (0.221)	−0.31 (0.157)
time of rise vs k_S	−0.09 (0.778)	−0.08 (0.802)	−0.06 (0.777)
duration vs A_S	−0.42 (0.172)	−0.32 (0.317)	−0.18 (0.403)
duration vs σ_S	−0.28 (0.371)	−0.18 (0.577)	−0.12 (0.577)
duration vs s_S	−0.14 (0.658)	−0.18 (0.585)	−0.15 (0.486)
duration vs k_S	−0.15 (0.638)	−0.14 (0.663)	−0.09 (0.676)
spotless days vs A_S	−0.74 (0.006)	−0.69 (0.013)	−0.57 (0.009)
spotless days vs σ_S	−0.81 (0.001)	−0.85 (0.001)	−0.69 (0.002)
spotless days vs s_S	−0.78 (0.003)	−0.75 (0.005)	−0.54 (0.014)
spotless days vs k_S	−0.48 (0.114)	−0.42 (0.174)	−0.24 (0.272)

Similar to Table 3, linear correlation coefficient r, a Spearman rank-order correlation value r_s, and Kendall's τ, calculated with the solar activity parameters and the statistical parameters of the latitudinal distribution of the observed sunspots only in the southern hemispheres.

northern hemisphere in that the chance probability is significantly high. The results are summarized in Tables 5 and 6. We have further calculated correlation coefficients between the statistical parameters obtained from one particular hemisphere and others from the other hemisphere or from both hemispheres. Generally speaking, combinations involving the the average latitude and the standard deviation end up with significantly correlated behavior. It turns out, however, that the skewness and and the kurtosis commonly result in uncorrelated relations, or that other correlations are insignificant with high rejection probabilities.

Finally, we attempt to address an effect of the sunspot size on the statistical behaviors. Conspicuous sunspots tend to show up around the solar maximum so that it is not so easy to find them in a long descending phase. Consequently, while the standard butterfly diagram is overwhelmed by small and numerous sunspots, larger and yet rare ones are apt to be distributed in a restricted regions of narrow latitude bands (Ternullo 2007; Chang 2011). For this reason, it is presumed that the latitudinal distribution of larger sunspots is inevitably affected. To make sure that this expectation becomes true, we classify the observed sunspots on the basis of its area and allocate the assorted sunspots into corresponding bins from the largest to the smallest sunspot. As one may predict, in a bin for small sunspots there is a multitude of sunspots while in a bin for large sunspots there are a few sunspots. In Figure 3, we show the latitudinal distribution from the different sample of sunspots acquired by replotting the butterfly diagram using information on the observed sunspot area during the sunspot cycles 12 to 23. From top to bottom, the distribution results from the sunspots in 60%, 70%, 80%, 90% of the number of bins counted in order from the top bin which is designated for the largest sunspot, respectively. In Figure 4, as an example of the latitudinal distributions of observed sunspots during an individual solar cycle, we show them resulting from the solar cycle 19.

With the different sample of sunspots in 40%, 50%, 60%, 70%, 80%, 90% of the number of bins counted in order from the top bin, we have reiterated the whole procedures up to recalculations of the correlation coefficients with the rejection probability between the solar activity parameters and the statistical parameters of the latitudinal distribution. It has been found that correlated tendency we discussed above is reproduced down to the data sets of the observed sunspots in 60% of the number of bins counted in order from the top bin. It should be stressed, however, that this aspect should be understood by the fact that 50% of the number of bins from the top bin comprises the sunspots less than a couple of percent of total number of sunspots. In other words, when one is reviewing the relation between the solar activity parameters and the statistical parameters of the latitudinal distribution for sets of the largest sunspots as done here, s/he is apt to find that the rejection probability becomes too high to propose any solid statistical conclusions. In this sense, we come to conclude that the statistical parameters of the latitudinal distribution seemingly correlate with the solar activity

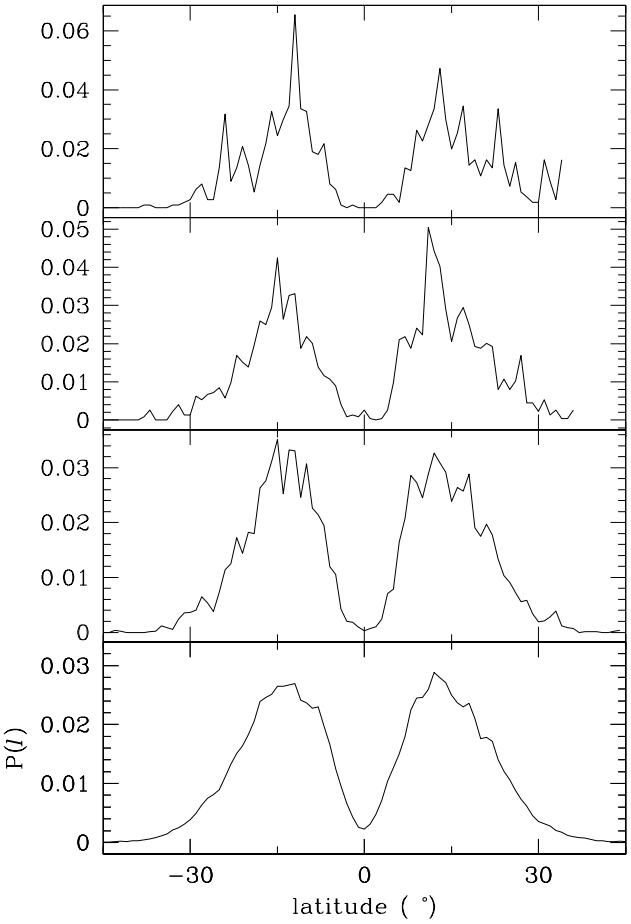

Figure 3. Latitudinal distributions from the different sample of sunspots acquired by replotting the butterfly diagram with assorted sunspots by size, which are observed during the sunspot cycles 12 to 23. From top to bottom, the distribution results from the sunspots in 60%, 70%, 80%, 90% of the number of bins counted in order from the top bin which is designated for the largest sunspot, respectively. The bins are assigned by sunspot area.

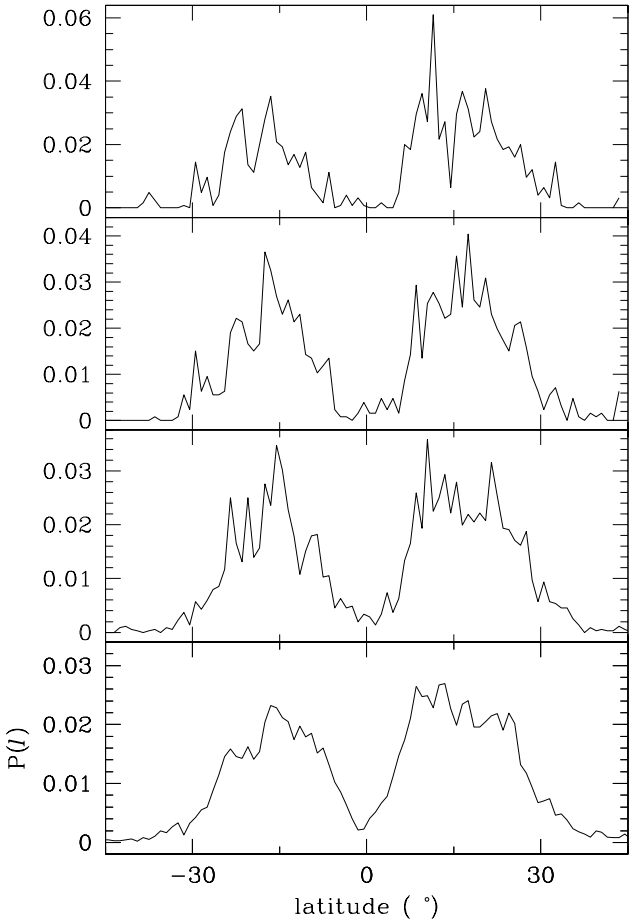

Figure 4. Similar to Figure 3, except that the sunspots are observed during the solar cycle 19.

parameters up to sizable sunspots, and that conclusions for the largest sunspots are drawn with due care. It is because this does not necessarily mean that largest sunspots are randomly scattered regardless of the level of solar activity.

5. SUMMARY AND CONCLUSIONS

The temporal and spatial distributions of the observed sunspots provide much information on the physical processes inducing the solar magnetic field's structure and evolution, as they immediately form when the magnetic tube emerges to the surface of the Sun. Investigating the latitudinal distribution of sunspots, we have attempted to establish a correlation between the statistical parameters of the latitudinal distribution of sunspots and characteristics of solar activity. For this purpose, we have statistically analyzed the daily sunspot areas and latitudes observed from May in 1874 to September in 2016. To see if the northern and southern hemispheres of the Sun behave rather differently, we have repeatedly carried out the whole analysis with the sunspots only appearing either in the northern hemisphere or in the southern hemisphere. We have also attempted to address a question of how the conclusion depends on the size of sunspots.

Our main findings are as follows:

(1) The maximum ISN strongly correlates with the mean number of sunspots per day, while the maximum ISN strongly anti-correlates with the number of spotless days. The mean number of sunspots per day strongly anti-correlates with the number of spotless days. The maximum ISN marginally anti-correlates with the total durations and the duration of ascending phase, and the number of spotless days also marginally correlates with not only the total durations but also the duration of ascending phase.

(2) The average latitude strongly correlate with both the standard deviation and the skewness, and the skewness also strongly correlate with both the standard deviation and the kurtosis. While, the kurtosis marginally correlate with the average latitude and the standard deviation.

(3) Both the maximum ISN and the mean number

of sunspots per day strongly correlate with the statistical parameters including the the average latitude, the standard deviation, the skewness, while they appears to marginally correlate with the kurtosis. The number of spotless days show similar behaviors, except that they are anti-correlated.

(4) For the sunspots observed in only one of either hemispheres, significant correlations between the average latitude and the standard deviation, and between the skewness and the kurtosis are recovered. The correlated behavior between the standard deviation and the skewness can be found from the sunspots appearing in the southern hemisphere, but not in the northern hemisphere.

(5) With the data sets of the observed the sunspots down to 60% of the number of bins counted in order from the top bin, the statistical parameters of the latitudinal distribution seemingly correlate with the solar activity parameters. As for the set of the largest sunspots the rejection probability is too high to draw any solid statistical conclusions.

Therefore, we propose that the mean number of sunspots per day and the number of spotless days are a good indicator of solar activity. One may conclude that for a strong solar cycle the profiles are peaked such that the latitudinal distribution is skewed closer to the equator while sunspots are distributed farther up to higher latitudes. It is also concluded that the statistical parameters of the latitudinal distribution seemingly correlate with the solar activity parameters up to sizable sunspots. It should be pointed out, however, that conclusions for the sample of the largest sunspots are drawn with due care.

Acknowledgments

The author thanks the anonymous referees for critical comments and helpful suggestions which greatly improve the original version of the manuscript. This study was supported by a National Research Foundation of Korea Grant funded by the Korean government (NRF-2018R1D1A3B070421880) and Basic Science Research Program through the National Research Foundation (NRF) of Korea funded by the Ministry of Science, ICT and Future Planning (No. 2018R1A6A1A06024970).

References

Carrington, R. C. 1860, On Dr. Soemmering's Observations Of The Solar Spots In The Years 1826, 1827, 1828, and 1829, MNRAS, 20, 71

Chang, H.-Y. 2011, Correlation Of Parameters Characterizing The Latitudinal Distribution Of Sunspots, New Astron., 16, 456

Chang, H.-Y. 2012, Bimodal Distribution of Area-weighted Latitude of Sunspots and Solar North-South Asymmetry, New Astron., 17, 247

Chang, H.-Y. 2015, Latitudinal Distribution Of Sunspots And Duration Of Solar Cycles, JKAS, 48, 325

Chang, H.-Y. 2018, Latitudinal Distribution Of Sunspot And North-South Asymmetry Revisited, J. Astron. Space Sci., 35, 55

Cho, I. H., Kwak, Y. S., Marubashi, K., et al. 2012, Changes In Sea-Level Pressure Over South Korea Associated With High-Speed Solar Wind Events, AdSpR, 50, 777

de Artigas, M. Z., Elias, A. G., & de Campra, P. F. 2006, Discrete Wavelet Analysis to Assess Long-term Trends in Geomagnetic Activity, Phys. Chem. Earth, 31, 77

Garcia, R. R., Solomon, S., Roble, R. G., & Rusch, D. W. 1984, A Numerical Response of the Middle Atmosphere to the 11-year Solar Cycle, P&SS, 32, 411

Gnevyshev, M. N., & Ohl, A. I. 1948, On the 22-year Cycle of Solar Activity, AJ, 38, 15

Gray, L. J., Ball, W., & Misios, S. 2017, Solar Influences On Climate Over The Atlantic/European Sector, AIP Conf. Proc., 1810, 020002

Haigh, J. D. 2007, The Sun and the Earth's Climate, Living Rev. Solar. Phys., 4, 2

Hale, G. E., Ellerman, F., Nicholson, S. B., Joy, A. H. 1919, The Magnetic Polarity of Sun-Spots, ApJ, 49, 153

Hathaway, D. H. 2011, A Standard Law for the Equatorward Drift of the Sunspot Zones, SoPh, 273, 221

Hathaway, D. H., & Wilson, R. M. 2004, What the Sunspot Record Tells Us About Space Climate, SoPh, 224, 5

Howard, R. F. 1991, Axial Tilt Angles of Sunspot Groups, SoPh, 136, 251

Javaraiah, J. 2007, North-South Asymmetry in Solar Activity: Predicting the Amplitude of the Next Solar Cycle, MNRAS, 377, 34

Joshi, B., Pant, P., & Manoharan, P. K. 2006, North-South Distribution of Solar Flares during Cycle 23, J. Astrophys. Astron., 27, 151

Joshi, B., Bhattacharyya, R., Pandey, K. K., et al. 2015, Evolutionary Aspects and North-South Asymmetry of Soft X-ray Flare Index during Solar Cycles 21, 22, and 23, A&A, 582, A4

Kane, R. P. 2005, Differences in the Quasi-biennial Oscillation and Quasi-triennial Oscillation Characteristics of the Solar, Interplanetary, and Terrestrial Parameters, JGRA, 110, A01108

Kim, J.-H., & Chang, H.-Y. 2019, Association between Solar Variability and Teleconnection Index, J. Astron. Space Sci., 36, 149

Krivova, N. A., & Solanki, S. K. 2002, The 1.3-year and 156-day Periodicities in Sunspot Data: Wavelet Analysis Suggests a Common Origin, A&A, 394, 701

Li, K. J. 2010, Latitude Migration of Solar Filaments, MNRAS, 405, 1040

Li, K. J., Liang, H. F., Yun, H. S., et al. 2002, Statistical Behavior of Sunspot Groups on the Solar Disk, SoPh, 205, 361

Li, K. J., Liang, H.-F., & Feng, W. 2010, Phase Shifts of the Paired Wings of Butterfly Diagrams, RAA, 10, 1177

Maunder, E. W. 1904, Note on the Distribution of Sun-spots in Heliographic Latitude, 1874–1902, MNRAS, 64, 747

Meehl, G. A., Arblaster, J. M., Matthes, K., et al. 2009, Amplifying The Pacific Climate System Response To A Small 11-Year Solar Cycle Forcing, Science, 325, 1114

Mironova, I. A., & Usoskin, I. G. 2013, Possible Effect Of Extreme Solar Energetic Particle Events Of September.October 1989 On Polar Stratospheric Aerosols: A Case Study, Atmospheric Chem. Phys., 13, 8543

Pevtsov, A. A., Berger, M. A., Nindos, A., et al. 2014, Magnetic Helicity, Tilt, and Twist, SSRv, 186, 285

Prestes, A., Rigozo, N. R., Echer, E., et al. 2006, Spectral Analysis of Sunspot Number and Geomagnetic Indices (1868–2001), J Atmos Sol Terr Phys, 68, 182

Pulkkinen, P. J., Brooke, J., Pelt, J., et al. 1999, Long-Term Variation of Sunspot Latitudes, A&A, 341, L43
Pudovkin, M. I., Veretenenko, S. V., Pellinen, R., et al. 1997, Meteorological Characteristic Changes In The High-Latitudinal Atmosphere Associated With Forbush Decreases Of The Galactic Cosmic Rays, AdSpR, 20, 1169
Roy, J. R. 1977, The North-South Distribution Of Major Solar Flare Events, Sunspot Magnetic Classes And Sunspot Areas (1955–1974), SoPh, 52, 53
Roy, I., & Haigh, J. D. 2010, Solar Cycle Signals In Sea Level Pressure And Sea Surface Temperature, Atmos. Chem. Phys., 10, 3147
Solanki, S. K., Wenzler, T., & Schmitt, D. 2008, Moments of the Latitudinal Dependence of the Sunspot Cycle: A New Diagnostic of Dynamo Models, A&A, 483, 623
Svensmark, H., & Friis-Christensen, E. 1997, Variation Of Cosmic Ray Flux And Global Cloud Coverage-A Missing Link In Solar-Climate Relationships, J Atmos Sol Terr Phys, 59, 1225
Temmer, M., Veronig, A., & Hanslmeier, A. 2002, What Causes the 24-Day Period Observed in Solar Flares?, A&A, 390, 707
Temmer, M., Rybák, J., Bendik, P., et al. 2006, Hemispheric Sunspot Numbers Rn and Rs from 1945–2004: Catalogue and N-S Asymmetry analysis for solar cycles 18–23, A&A, 447, 735
Ternullo, M. 2007, The Butterfly Diagram Fine Structure, SoPh, 240, 153
Ternullo, M. 2010, The Butterfly Diagram Internal Structure, Ap&SS, 328, 301
Tinsley, B. A. 2000, Influence Of Solar Wind On The Global Electric Circuit, And Inferred Effects On Cloud Microphysics, Temperature, and Dynamics In The Troposphere, SSRv, 94, 231
Usoskin, I. G. 2017, A History Of Solar Activity Over Millennia, Living Rev. Solar. Phys., 14, 3
Verma, V. K. 1987, On the increase of solar activity in the Southern Hemisphere during solar cycle 21, SoPh, 114, 185
Verma, V. K. 1993, On The North-South Asymmetry Of Solar Activity Cycles, ApJ, 403, 797
Waldmeier, M. 1935, Neue Eigenschaften der Sonnenfleckenkurve, Astron. Mitt. Zurich, 14, 105
Waldmeier, M. 1971, The Asymmetry Of Solar Activity In The Years 1959–1969, SoPh, 20, 332
Wang, Y.-M., & Sheeley, N. R. Jr. 1989, Average Properties Of Bipolar Magnetic Regions During Sunspot Cycle 21, SoPh, 124, 81
White, O. R., & Trotter, D. E. 1977, Note On The Distribution Of Sunspots Between The North And South Solar Hemispheres And Its Variation With The Solar Cycle, ApJS, 33, 391
Zaatri, A., Komm, R., Gonzalez Hernandez, I., et al. 2006, North South Asymmetry of Zonal and Meridional Flows Determined From Ring Diagram Analysis of Gong ++ Data, SoPh, 236, 227
Zharkova, V. V., & Shepherd, S. J. 2022, Eigenvectors of Solar Magnetic Field in Cycles 21–24 and Their Links to Solar Activity Indices, MNRAS, 512, 5085
Zolotova, N. V., & Ponyavin, D. I. 2006, Phase Asynchrony of the North-South Sunspot Activity, A&A, 449, L1
Zolotova, N. V., & Ponyavin, D. I. 2007, Was the Unusual Solar Cycle at the End of the XVIII Century a Result of Phase Asynchronization?, A&A, 470, L17